PROCEEDINGS, 49th Workshop on Geothermal Reservoir Engineering
Stanford University, Stanford, California, February 12-14, 2024
SGP-TR-227

Geologic Assessment of Four Greenfield Sites for Solar-Geothermal Hybrid Power Plants

Ghanashyam Neupane[1,2], Daniel S. Wendt[1], Joshua D. McTigue[3], and Juliet G. Simpson[3]

[1]Idaho National Laboratory, Idaho Falls, ID 83415

[2]Center for Advanced Energy Studies, Idaho Falls, ID 83401

[3]National Renewable Energy Laboratory, Golden, CO80401

Email: ghanashyam.neupane@inl.gov

Keywords: Hybrid geothermal, geo-solar, low temperature geothermal, Castle Creek, Elk Hills, McGregor Range, Cranfield

ABSTRACT

Power generation from low to medium temperature geothermal resources, including conventional hydrothermal systems and oil & gas producing reservoirs with elevated temperatures, can help stabilize the electric grid with increasing power contributions from variable renewable resources. But the generation of power from the low to medium temperature geothermal resources are costly because of poor thermal efficiencies. To overcome this technoeconomic barrier, these sub-par geothermal resources could be hybridized with other sources of thermal energy such as concentrating solar and natural gas and make them more competitive and attractive for power generation. In addition, hybridization could expand the potential geothermal resource areas, which are mostly distributed in the western part of the US to several other regions in the country. In this work, we selected four low to medium temperature geothermal resources in Idaho, California, New Mexico, and Mississippi and investigated hybridization of these resources with different potential for concentrating solar heating for competitive power generation. Two of the sites, Grand View in Idaho and McGregor Range in New Mexico are conventional low-temperature hydrothermal resource areas with low and high concentrating solar heating potential, respectively. The other two sites, Elk Hills in California and Cranfield in Mississippi, are currently and previously oil and gas producing reservoir systems of elevated temperatures with high and low concentrating solar heating potential, respectively. This paper presents the geology, hydrology, and geochemical characteristics of these selected sites and summarizes the preliminary modeling results of hybridized power generation with concentrating solar heating technology.

1. INTRODUCTION

The contribution of renewable energy, particularly from variable resources, to the electrical grid is increasing as a measure to minimize the climate change effects from greenhouse gas emissions from the use of fossil fuels as major energy sources. However, the renewable energy from variable resources such as solar and wind introduce instability in the grid. For grid stability, energy contribution from a consistent baseload power, desirably from a renewable source, is needed. Unlike other variable resources, geothermal energy, which harnesses thermal energy stored in the earth's crust, can provide baseload power, and help maintain grid stability. However, the main challenge in increasing the market share of geothermal power, especially from the low to medium temperature geothermal resources, is relatively low thermal efficiency and higher generation costs compared to wind and solar.

One of the approaches to increase efficiency for geothermal resources with low to medium temperatures is to couple it with other resources. An ongoing research effort at INL and NREL is evaluating hybridization of low to medium temperature geothermal resources with concentrated solar heat for generation of power through binary power plants (Wendt et al., 2023; McTigue et al., 2023). This approach provides several attributes that may allow geothermal power plants to generate power at more competitive cost. First, the addition of solar thermal energy input to a geothermal power plant provides additional heat input that can be converted to electrical power. Second, the temperature level of the heat obtained from concentrating solar collectors is higher than that of geothermal heat, which provides opportunities for improving the efficiency of the conversion of thermal energy to electrical power. Thirdly, solar heat is amenable to energy storage to provide increased power generation during periods of peak demand. The hybrid plant dispatchability and power output can be further increased by including natural gas combustion which would effectively create a system that could provide both baseload and peaking power.

For the evaluation of the solar topping hybridization technology for geothermal power generation, several low to medium temperature geothermal resource areas with different solar energy potentials were selected. This paper represents a part of the overall project to evaluate the technology and economic viability of geo-solar hybridization technology. In this paper, we provide geological, hydrological, and geochemical (scaling of the brines) characteristics as well as include a summary of the hybrid geo-solar power generation modeling results for these case study sites.

2. CASE STUDY SITES

2.1 Site Selection Criteria

Four low to medium temperature geothermal resource areas were selected for this study. The selected sites are in Idaho, California, New Mexico, and Mississippi. The main criteria to select these sites for this study are 1) diversity in geographic areas, 2) geothermal resource grades, and 3) solar resource grade. Also, availability of coexisting natural gas played a minor role in selection of the sites.

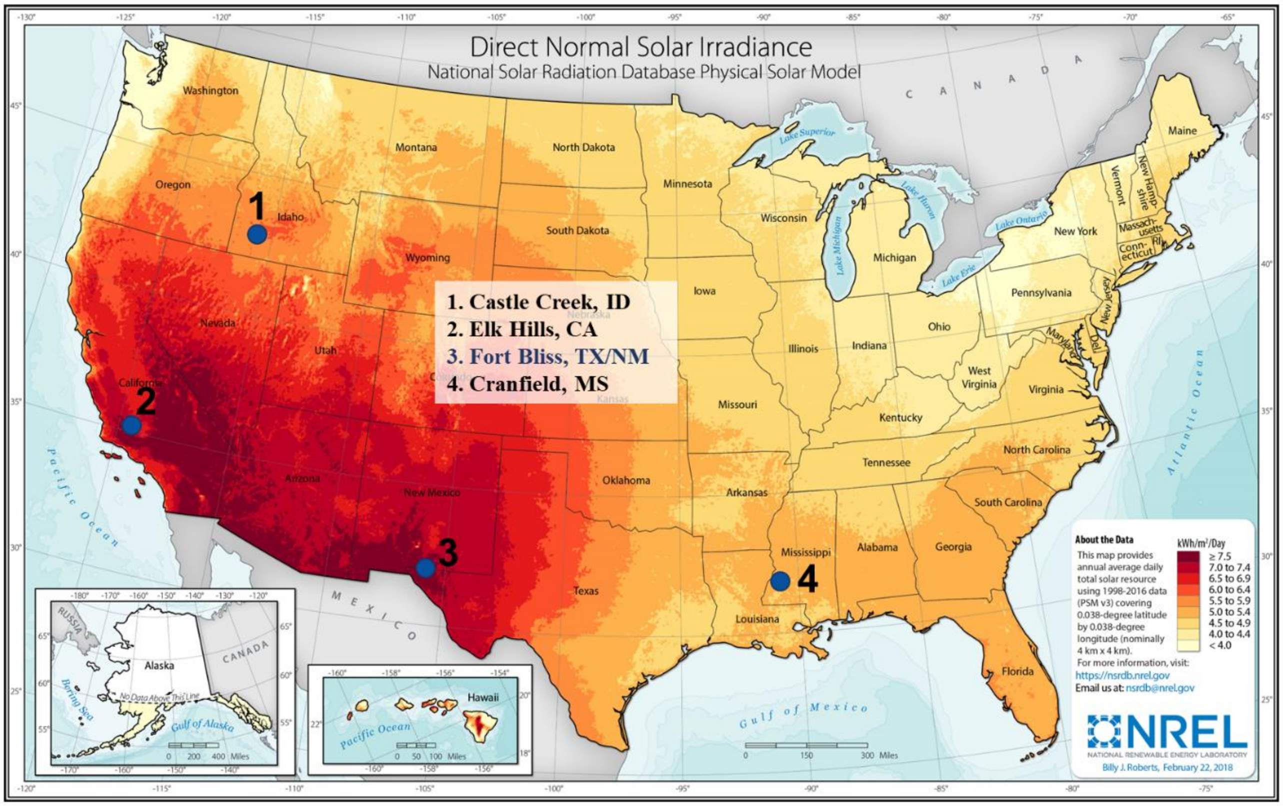

Figure 1. Selected study sites plotted on direct normal solar irradiance map of the conterminous United States.

In the United States, most of the identified geothermal resources are in the western part of the country. For this study, we were also interested in evaluating geothermal resources in the southeastern part of the country for their economic viability with concentrated solar hybridization. Although all case study sites are of low to medium temperature geothermal resources in conventional terms, we have subdivided them into two categories for this study as low-temperature (90 to 120°C) and high-temperature (120 to 150°C) systems to evaluate the impact of concentrating solar hybridization on geothermal resources of different temperatures. The selected sites also represent diverse solar resource grades (Figure 1). Some of the study sites are categorized as having low-irradiance (<6.4 kWh/m^2/day) and high-irradiance (>6.5 kWh/m^2/day) in terms of solar heat potential. The qualitative categories of the geothermal and solar grades for the selected sites are given in Table 1. Two of the selected sites, the Elk Hills in California and the Cranfield site in Mississippi have availability of locally produced natural gas as a potential additional heat source. Salient characteristics of all selected sites are given in Table 2. It is noted here that the number of wells required to generate 10 MWe of power is only from the stand-alone geothermal resources (non-hybrid).

Table 1: Geothermal and solar resource grades of the selected sites

		Solar	
		Low	High
Geothermal	Low	Castle Creek, ID	Fort Bliss, NM
	High	Cranfield, MS	Elk Hills, CA

Table 2. Characteristics of selected case study sites

Sites		Castle Creek	Elk Hills	McGregor Range	Cranfield site
Latitude		42.96333	35.280115	32.068639	31.563533
Longitude		-116.076655	-119.469009	-106.155008	-91.141487
State		Idaho	California	New Mexico	Mississippi
Geothermal	Measured temp (°C)	108	89.5 @ 2250 m* 135 @ 2800 m	96	127
	Injection temp (°C)	51	52	51	51
	Province/Basin	Snake River Plain	San Juaquin	Tularosa Basin	Gulf Coast
	Resource depth (m)	2672	2225 2800	1500	3100
	Reservoir pressure, psi	213	3200 3645	1918	4641
	Pumping power (kWe/MWe)	181	125	284	98
	Resource grade	Low	Low to High	Low	High
	Geology	Sedimentary, volcanics	Sedimentary	Sedimentary, intrusive	Sedimentary
	Reservoir rock	Rhyolite	Sandstones	Carbonates	Sandstones
	Drilling difficulty	Low-Medium	Low-Medium	Low	Low
	Brine chemistry	<1000 mg/L TDS	<50,000 mg/L TDS; low sulfate	~10,000 mg/L TDS; sulfate rich	150K mg/L TDS, low sulfate
	Qualitative permeability	High	Low-Medium	Commercial	Medium
	Flow rate/well or hot springs (gpm)	1000	2000 1300	1000	2000
	# Prod well for 10 MWe	8	4	12	2
Solar	Resource grade	Low	High	High	Low
	Direct Normal Irradiance ($kWh/m^2/day$)	5.7	6.6	7.1	5
Other energy source		Wind	Natural gas		Natural gas
Drilling cost estimates per well (in millions as 2020 US $)		6.8	5.5/7	4.9	7.3

*The gray font data for the Elk Hills area are for a shallower secondary reservoir.

2.2 Case Study Sites

2.2.1 Castle Creek, Idaho

The Snake River Plain (SRP) in southern Idaho has long been recognized as an area with high heat flow and geothermal potential (e.g., Brott et al., 1978; Blackwell, 1989). Several areas within and along the margins of the SRP were previously marked as Known Geothermal Resource Areas (KGRA), including the Castle Creek area in Owyhee County in southwestern Idaho. The geothermal resource potential of this area is manifested by several hot springs and thermal wells in (Figure 2). The average direct normal solar irradiance at this site is 5.7 $kWh/m^2/day$.

The stratigraphy of this area consists of surficial alluvial deposits followed by a series of Pleistocene flood basalts. These younger basalts are more prominent in the northern part of the area, particularly, north of the Snake River. Underlying the younger basalts and alluvial deposits are sediments of the Idaho Group, consisting of a suite of 252-680 m thick lacustrine sediments ranging from clays to sands to gravels, with intercalated limestones as well as basaltic and silicic tuffs. These fine-grained sediments are exposed extensively in the area and were deposited in the Lake Idaho basin. There is a thick (134-377 m) sequence of basalts that underlie these sediments, and are often called the Banbury Basalt, and have been interpreted to be 7-9 Ma in age (Young and Whitehead, 1975; Wood and Clemens, 2002). These basalts in turn overlie a thick sequence (up to 2329 m) of Miocene silicic volcanic rocks, known collectively as the Idavada Volcanics (Young and Whitehead, 1975). Most of the deeper wells in the area bottom out in the Idavada volcanics, and this unit is considered as the deeper geothermal reservoir. The deepest well in the area, the Anschutz Federal 60-13 No. 1, bottoms out in the Cretaceous granitic rocks similar to the granite-granodiorite rocks encountered in central Idaho batholith region (Mariner et al., 2006).

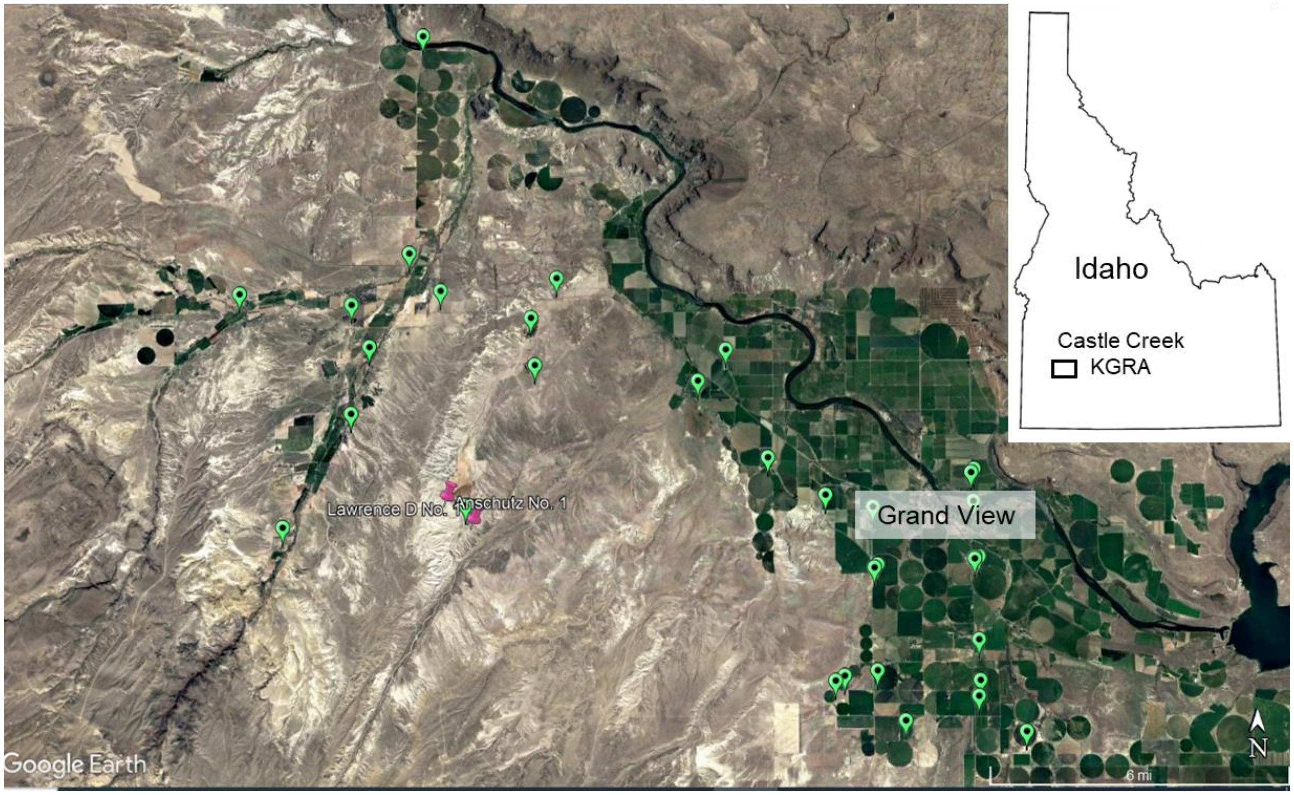

Figure 2. (A) Castle Creek geothermal area around Grand View, Idaho, (B) Distribution of hot springs and (thermal) wells in the area. Two deep wells, Lawrence D No. 1 (2672 m) and Anschutz No. 1 (3391 m) with bottom hole temperatures of 108°C and 149°C, respectively.

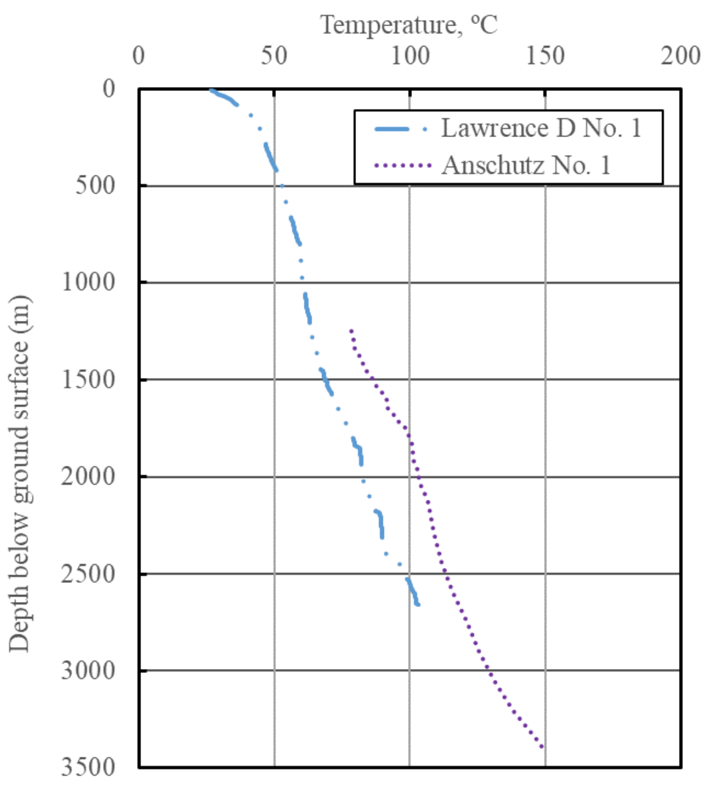

Figure 3. Temperature profiles along two deep wells in the Castle Creek KGRA near Grand View, Idaho.

Figure 3 shows measured temperature profile along two deep wells in the area. The maximum recorded temperature in the area is 149º C measured at the bottom of the Anschutz Federal 60-13 No. 1 well. Another deep well (Lawrence D No. 1) in the area, however, only recorded a measured bottomhole temperature of 108º C. For this study, 108°C is used as the geothermal resource temperature for the Castle Creek case. Since the bottomhole temperature of the well Lawrence D No. 1, which was drilled to confirm the geothermal resource, was deemed low for the prevailing conventional geothermal technology, Phillips Petroleum ceased the additional geothermal exploration in the area and both wells were subsequently abandoned in the early 1980s. Although the two deeper geothermal wells were abandoned, the area has numerous thermal wells producing hot water up to temperatures of 83º C from the Idavada Volcanics-hosted geothermal aquifer. Thermal water in the area is generally under artesian conditions, and reportedly sustains over 1,000 gallons/min flow in many wells (Young and Lewis, 1982). The likely reservoir thickness including the Idavada Volcanics and underlying silicic unit is not known, but it could be several hundreds of meters. In Table 2, a reservoir thickness of about 150 m is given to represent a section of the larger geothermal reservoir at a depth of about 2,672 m. The permeability of this reservoir is 3000 millidarcies, a geometric mean value of permeability for Idavada Volcanics-hosted aquifer system in Bruneau area (Adkins and Bartolino, 2012).

2.2.1 Elk Hills, California

The Elk Hills oil field in the southern San Joaquin Valley is about 30 kilometers southwest from Bakersfield in Kearn County, California. Most of the Elk Hills field was previously designated as the Naval Petroleum Reserve No. 1 (Woodring et al., 1932), and it represents one of the most productive oil and gas basins in the country (Maher et al., 1975).

Stratigraphically, the area consists of thick sequences of shale and turbidites containing intervals of sandstones deposited in a forearc basin from the late Cretaceous to Pleistocene (Reid, 1995; Gautier et al., 2007). The five sandstone intervals present in the area are the primary reservoirs used to produce oil & and gas since oil was discovered in the area in early 1900s (Woodring et al., 1932; Maher et al., 1975; Reid, 1995). Structurally, the Elk Hills oil field consists of a series of northwest trending anticlines (Reid, 1995).

A few previous studies (e.g., Kharaka et al., 1981; Sanyal et al., 1993; Williams et al., 2004) have assessed the geothermal potential of sedimentary basins in California, including the Elk Hills field. Particularly, the geopressured oil & gas reservoirs with elevated temperatures are identified as areas with higher geothermal potential (Kharaka et al., 1981; Sanyal et al., 1993). Although the continuous production of oil & gas from these reservoirs has perturbed the pressure regime, the thermal regime of these systems has remained unchanged and can be developed for geothermal power generation with suitable technology (Williams et al., 2004).

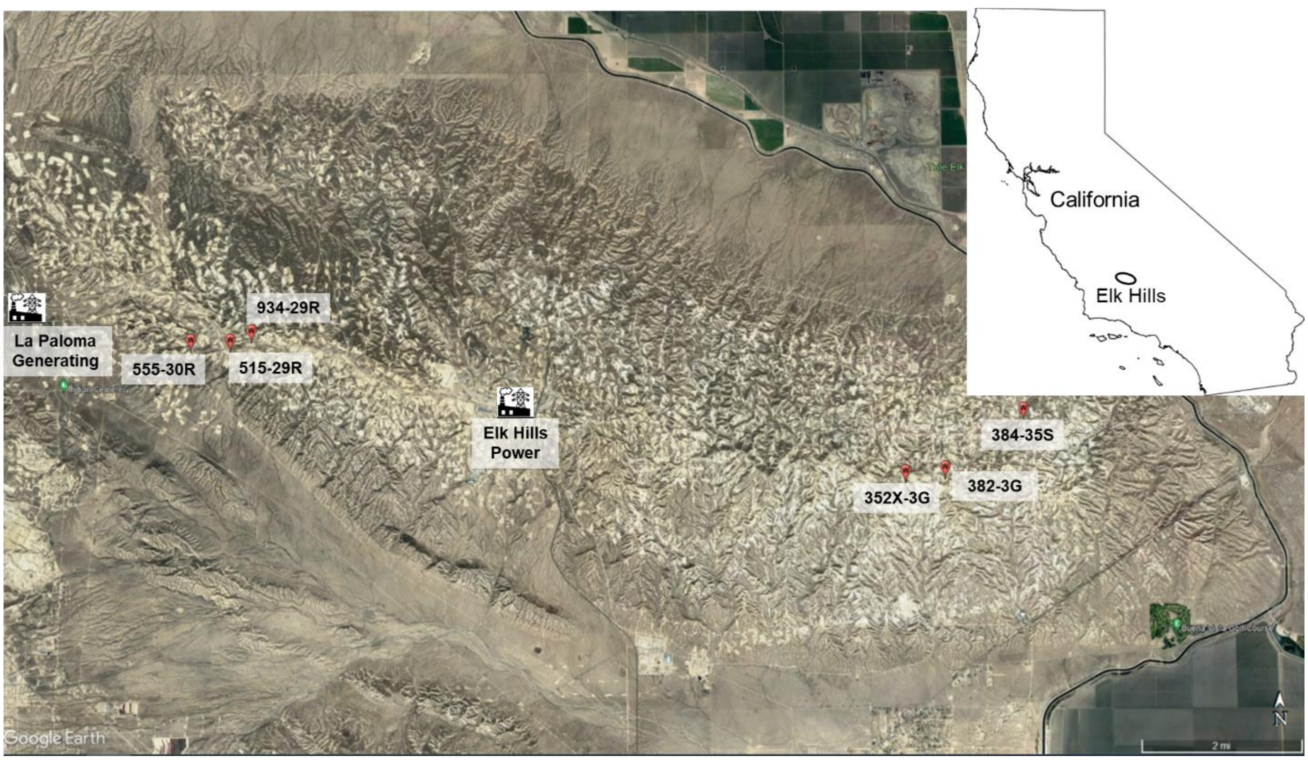

Figure 4. Elk Hills oil & gas field in San Joaquin valley, California showing locations of a few selected deep wells. The field has over a thousand wells in the area to produce oil & gas.

For this study, two sandstone sequences in the Elk Hills field – the Carneros Sandstone Member within the Oligocene-Miocene Temblor Formation and the Stevens Sandstone Member within the Miocene Monterey Formation – are identified as potential geothermal resources. In the western part of the Elk Hills, the Carneros Sandstone Member consists of three sandstone sequences with a total thickness of up to 290 m (950 ft) (Maher et al, 1975). However, these sandstone sequences wedge out towards east reaching about 100 m (~300 ft) at well 515-29 R. The temperature profile (Figure 5A) of the Carneros Sandstone in the western part of the Elk Hills is obtained from data collected along the Well 934-29R. The Carneros Sandstones generally have low permeability with about 14 millidarcys. The likely reservoir temperature in the Carneros Sandstone reservoir is about 135° C at about 2800 m (~9200 ft). The direct normal irradiance around the Elk Hills area is 6.6 kWh/m^2/day. The geothermal resource hosted in the Carneros Sandstone was used for evaluating its power generation potential with geo-solar hybrid technology.

The Stevens Sandstone consists of lenticular to tabular sheet sandstones and thick intervals of fractured siliceous shale. Main Body B sandstone beds are included within the Stevens. These sandstone beds are thick sheet sandstones. In well 382-3G (Figure 4), these beds are encountered within a depth range of 7109.5 to 7693.5 ft with an average porosity of 22 percent and an average permeability of 210 millidarcys (Maher et al., 1975). A temperature log (Figure 5B) is constructed using temperature log produced by Schlumberger in Well 352X-3G (Figure 4) for Union Oil in 1989. The highlighted portion of the temperature profile in Figure 5B is for the Main Body B sandstones of the Stevens Sandstones in the area showing a reservoir temperature of about 89° C.

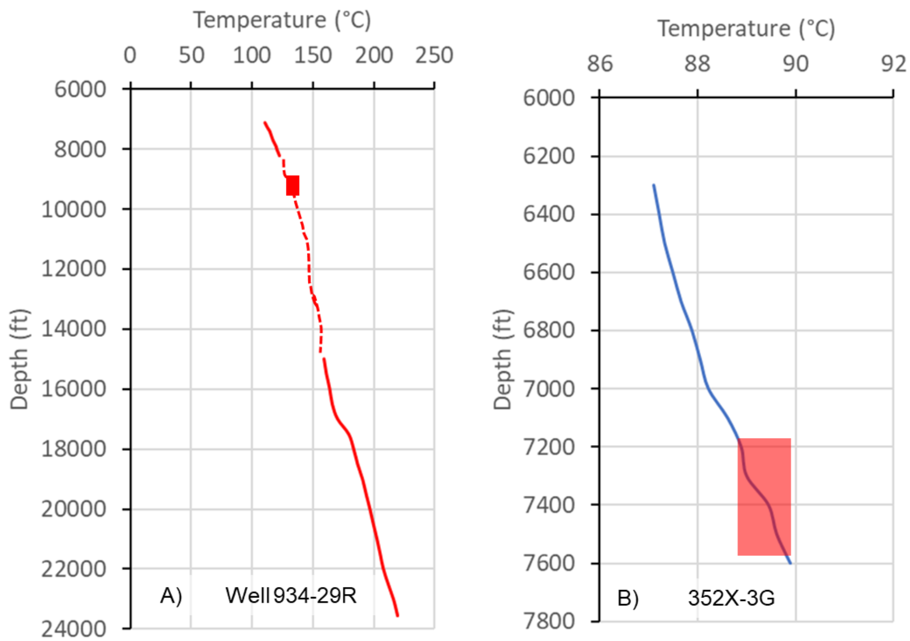

Figure 5. Vertical temperature profiles along the well 934-29R (A) and well 353X-3G (B). Temperature measurement data retrieved from CalGEM's well data repository.

2.2.3 McGregor Range, New Mexico

McGregor Range geothermal area in Otero County, New Mexio is about 45 km northeast from El Paso, Texas (Figure 6). The specific site selected for this study is an area around McGregor Range Basecamp, a military area (Figure 6B). This geothermal area further extends to the south into El Paso County, Texas where some hot springs expressions are present around the Hueco Tanks State Park area (Henry and Morton 1982; Roy et al., 1983). Geographically, the area is in the southeastern margins of the Tularosa-Hueco basin in the Rio Grande Rift (Nash and Bennett, 2015). The tectonic activities of orogeny and rifting in the area has resulted in a faulted geothermal reservoir with high-heat flow (Taylor et al., 1979; Lear et al., 2016). Previously, the geothermal resources in the Tularosa-Hueco basin area were investigated by several researchers (e.g., Taylor et al., 1979, 1980; Henry and Morton 1982; Roy et al., 1983; Lohse and Icerman, 1980; Nash and Bennett, 2015; Barker et al., 2015) for various applications including electrical power, direct-use, and ground-coupled heat pump.

Earlier investigations by Sandia National Laboratory (Finger and Jacobson, 1997) and Ruby Mountain Inc (Lear et al., 2016) provide detailed subsurface geology and characteristics of the geothermal reservoir around McGregor Range Basecamp. The Sandia led effort involved drilling of four exploratory wells with a primary goal of evaluating the geothermal resources around the basecamp for power generation and a secondary goal for direct use applications (Finger and Jacobson, 1997). Later in 2015, Ruby Mountain Inc drilled a geothermal-production scale well and conducted pumping tests to evaluate the economic viability of the resources for power generation.

Geologically, the area consisted of Quaternary surficial deposits, Paleozoic sedimentary sequences, primarily, carbonates and shales, and Precambrian basement rocks. Tertiary intrusions as sills are encountered at different depth levels in several wells in the area (Lear et al., 2016). The Silurian limestone and Ordovician dolostone are identified as the geothermal reservoir in the area at depth >915 m. Several faults (Figure 6B) associated with the Cenozoic extension of the Basin and Range Province are controlling the deep circulation in the area. Measured temperatures in several exploration wells in the area indicate the highest reservoir temperature in the area is 96 °C (Lear et al., 2016). Geothermometric temperature estimates based on the chemical composition of water produced from deep exploration wells indicate reservoir temperature as high as 121°C. In 2013, Ruby Mountain Inc conducted flow tests in Well 56-5 (Figure 6B) and concluded that the reservoir has a commercial grade permeability with potential to produce electricity with the existing technology and meet power need of the nearby McGregor Range Basecamp (Lear et al., 2016). This area has a higher direct normal irradiance of 7.1 kWh/m^2/day.

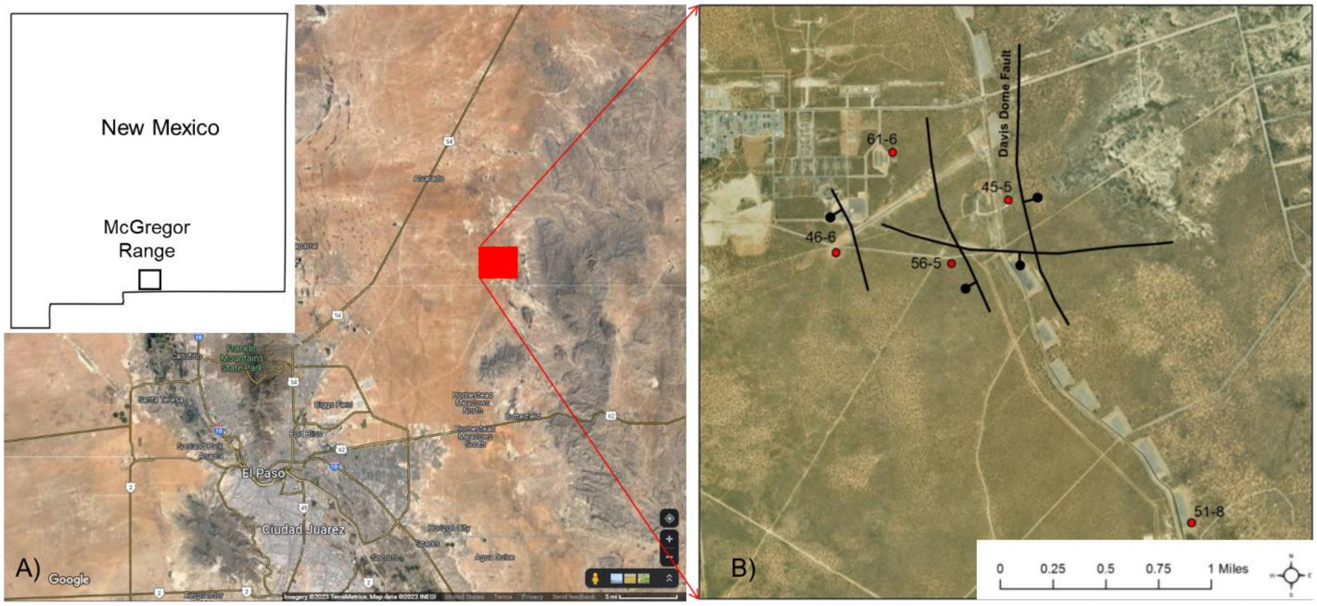

Figure 6. (A) McGregor Range geothermal area in south New Mexico and northeast from El Paso, Texas. (B) McGregor Range military basecamp and wells (Lear et al., 2016).

2.2.4 Cranfield, Mississippi

The Cranfield site is in Franklin County, Mississippi (Figure 7). The area around this site is a depleted oil & gas producing basin with a history of production of oil, condensate, and methane between 1944 and 1966. Lately, the Cranfield site was used as a carbon sequestration pilot for the Southeast Regional Carbon Sequestration Partnership (SECARB) (Riestenberg and Gray, 2009) and a test case for the thermal energy storage reservoir (McLing et al., 2022).

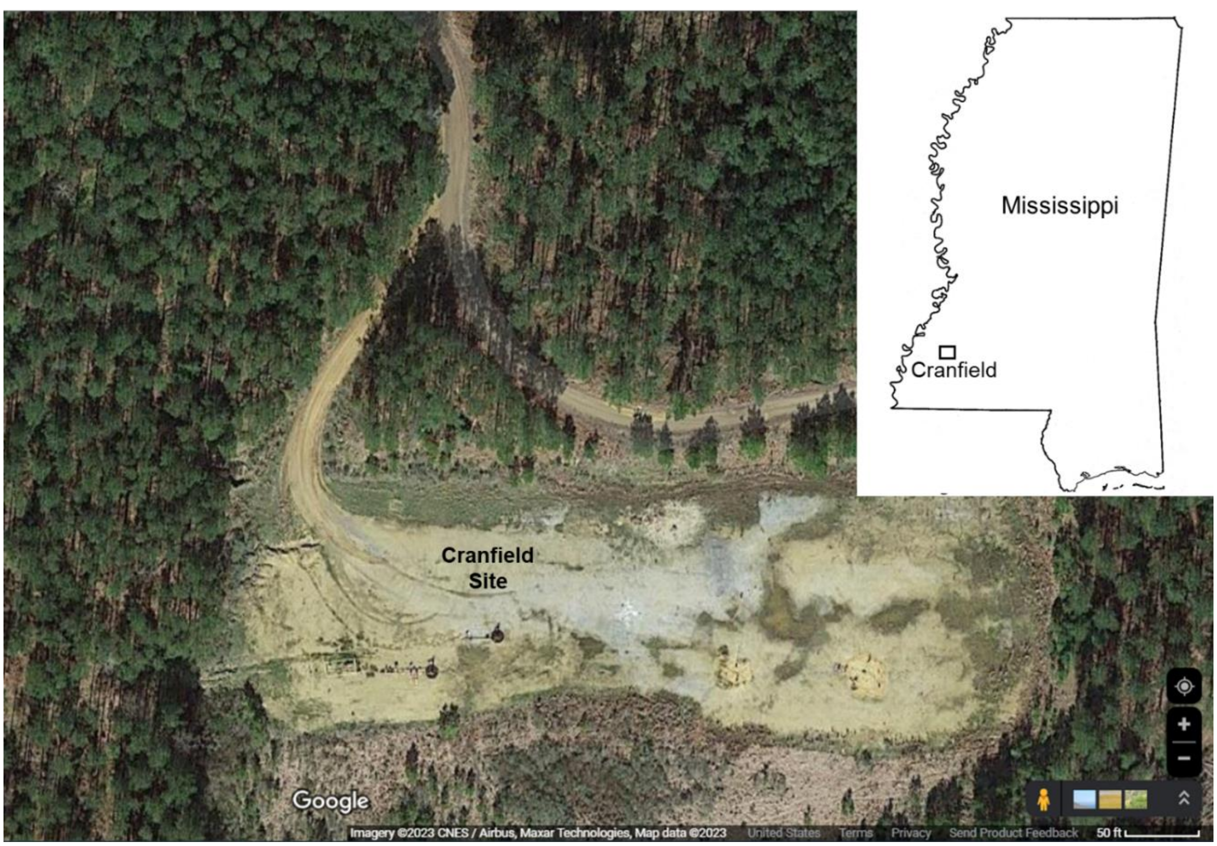

Figure 7. Cranfield site in Mississippi showing with well installations for carbon sequestration work.

As with the carbon sequestration pilot, the Upper Cretaceous Lower Tuscaloosa Formation is considered as the main geothermal reservoir for this study. Structurally, the area is a shallow-dipping domal feature created by a deep-seated inactive salt dome (Hosseini et al., 2013). The targeted reservoir at the site is up to 25 m in thickness at 3,100 m depth (Lu et al., 2012). The Lower Tuscaloosa Formation consists of a package of upward-fining depositional cycles of cross-bedded conglomerates, fine-grained sandstones, and muddy sandstone deposited in a fluvial-deltaic system (Lu et al., 2012).

Hydrogeologically, the reservoir is vertically heterogeneous but horizontally homogeneous with reported porosities of 0.7 to 0.33 and permeabilities of 0.03 to 423 millidarcies (Doughty and Freifeld, 2013). The reservoir is characterized as a hypersaline aquifer (Spycher et al., 2021). The measured reservoir temperatures in the wells range from 125 to 129 º C at the site, and a temperature of 127 º C was used as the geothermal resource temperature to evaluate the geo-solar technology. This area has a relatively lower direct normal irradiance of 5 kWh/m^2/day.

2.3. Brine Chemistry and Scaling Potential

Chemical composition of brines of the selected sites are assembled from literature (e.g., Young and Whitehead, 1975; Young and Lewis, 1982; Lear et al., 2016; Maher et al., 1975; Gans et al., 2019; Spycher et al., 2021) and presented in Table 3. Geothermal water in the Castle Creek area contains a low concentration of dissolved constituents whereas the fluid in the Cranfield site is hypersaline in nature. Brines in the Elk Hills and McGregor Range areas are intermediate in salinity containing several thousands of milligrams of dissolved solutes. A reaction path modeling of the brine compositions in Table 3 was conducted using the Geochemist's Workbench in terms of temperature from 200º C to 50º C to simulate the cooling effect during heat extraction in the heat exchanger.

Table 3. Representative composition of geothermal brines at the selected sites.

Sites	WellName	Temp (C)	pH	Al	Ca	Mg	Na	K	SiO_2(aq)	HCO_3	F	Cl	SO_4
Castle Creek	Lawrence Well #2	64.9	9.44	0.210	1.09	1	114	1	86.5	168	15.9	12.3	43
Castle Creek	Cooke Greenhouse Well #1	82.9	9.57	0.078	1.34	1	139	1.6	125.7	178	15.8	13.6	80
Castle Creek	George King	76.4	9.56	0.105	1	1	112	1	80.5	165	13.5	11.7	39
McGregor	Well 56-5_1250ft	86	6.49		305	51.7	2,680	117	41.8	173	4.4	4,220	846
McGregor	Well 56-5_2960ft	93	7.06		371	52.2	2,600	118	18.5	309	4.0	4,270	834
McGregor	Well 45-5_3135ft	83	6.8		480	98.9	3,570	228	61.4	375	3.5	5,298	1,054
Elk Hills	382-3G	90	7.1		1,011	300.5	9,974			253.2		17,849	42
Elk Hills	555-30R	135	8.03		24	7.1	6,166			2971		7,779	67
Cranfield	Unknown	127	5.46		12,400	1,090	46,000	433		315		96,900	250

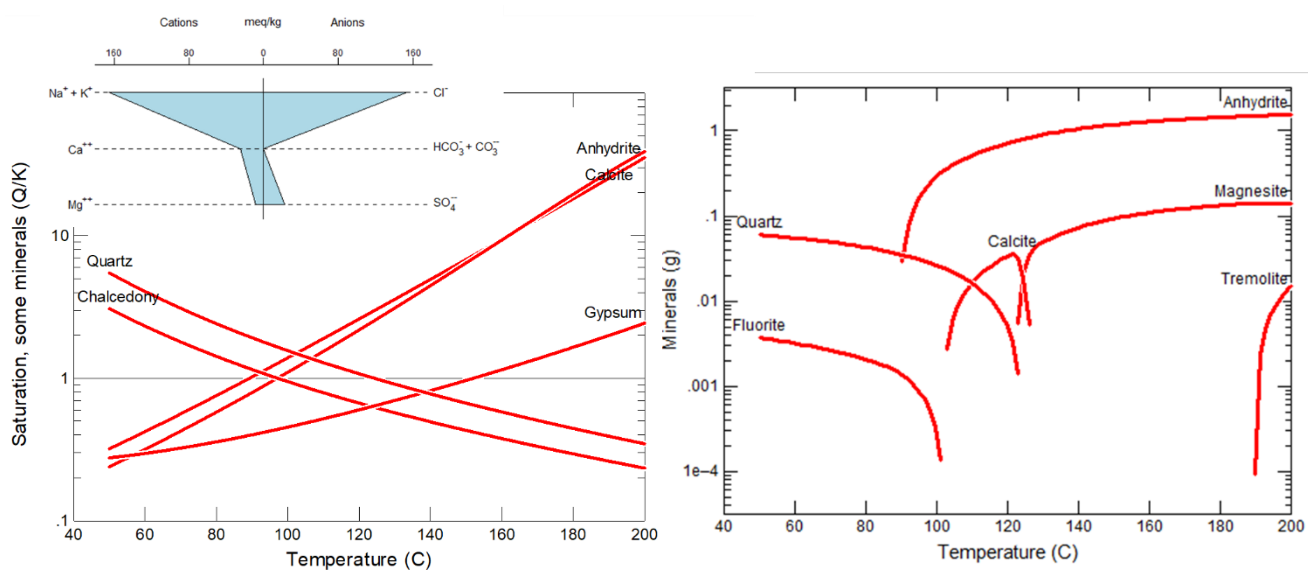

Figure 7. Geochemical modeling results for the McGregor Range site (Sample: Well 45-5_3135ft).

Figure 7 shows the geochemical modeling results for a representative McGregor Range geothermal brine sample. The reservoir temperature of this system is 96º C. Upon cooling (heat extraction), the brine sample becomes oversaturated with respect to quartz and silica, however, the brine is undersaturated with respect to amorphous silica. Since the solubility of silica at lower temperature is primarily controlled by amorphous silica, this brine is likely to create less scaling issue during heat extraction. Another example of geochemical modeling results is shown in Figure 8 for the Cranfield site (with reservoir temperature of 127º C. Again, the scaling potential for the hypersaline brine of the Cranfield site upon cooling is also minimum. Similarly low scaling potential during heat extraction is observed for the brines from the Castle Creek and Elk Hills sites.

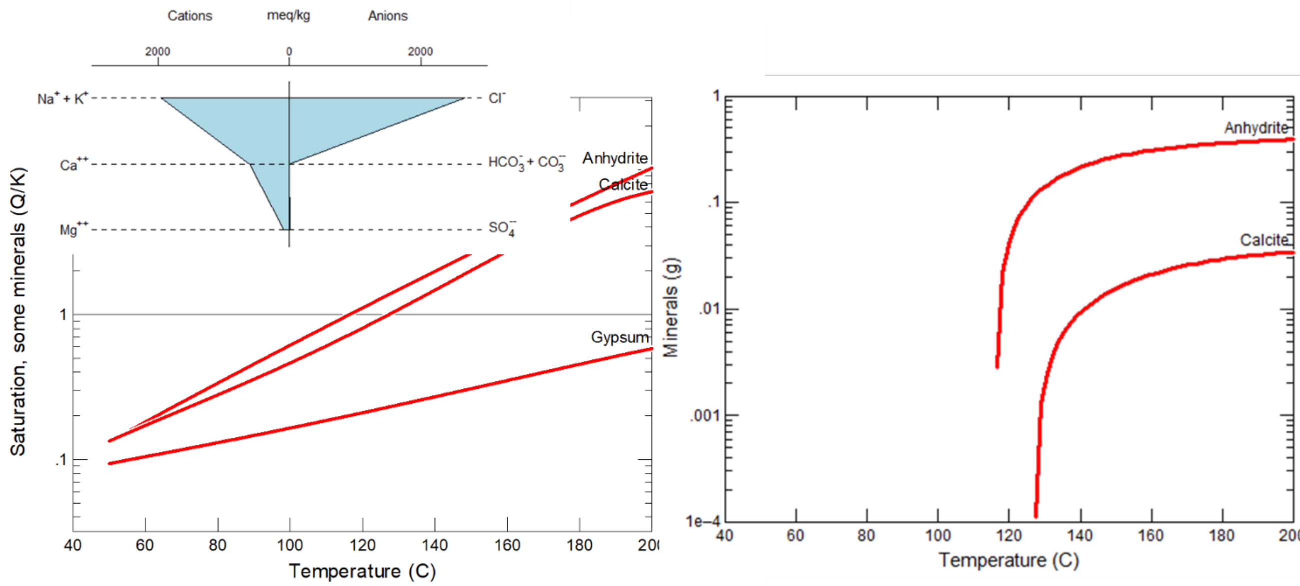

Figure 9. Geochemical modeling results for the Cranfield site.

3. ESTIMATION OF DRILLING COSTS

One of the major geothermal development costs is associated with drilling production and injection wells. The cost for drilling at a geothermal site is mostly related to the depth of the reservoir and type of rocks (Shamoushaki et al., 2021). The selected four case study sites are mostly of sedimentary types with volcanics (at Castle Creek) and intrusive (McGregor Range) rocks. General drilling cost of geothermal wells at each site was estimated using an empirical relationship represented in Figure 8. The estimated drilling cost at the Castle Creek, Elk Hills, McGregor, and Cranfield sites are 6.8, 7, 4.9, and 7.3 million dollars (2020-dollar value) per well, respectively. As seen in Figure 8, the drilling cost values for various US locations are scattered. The variation in drilling costs is attributed to many practical elements in well drilling and site-specific features (Shamoushaki et al., 2021). Therefore, the drilling costs obtained from the model presented in Figure 8 need to be considered as tentative estimates, and the actual drilling cost at each site is likely to vary.

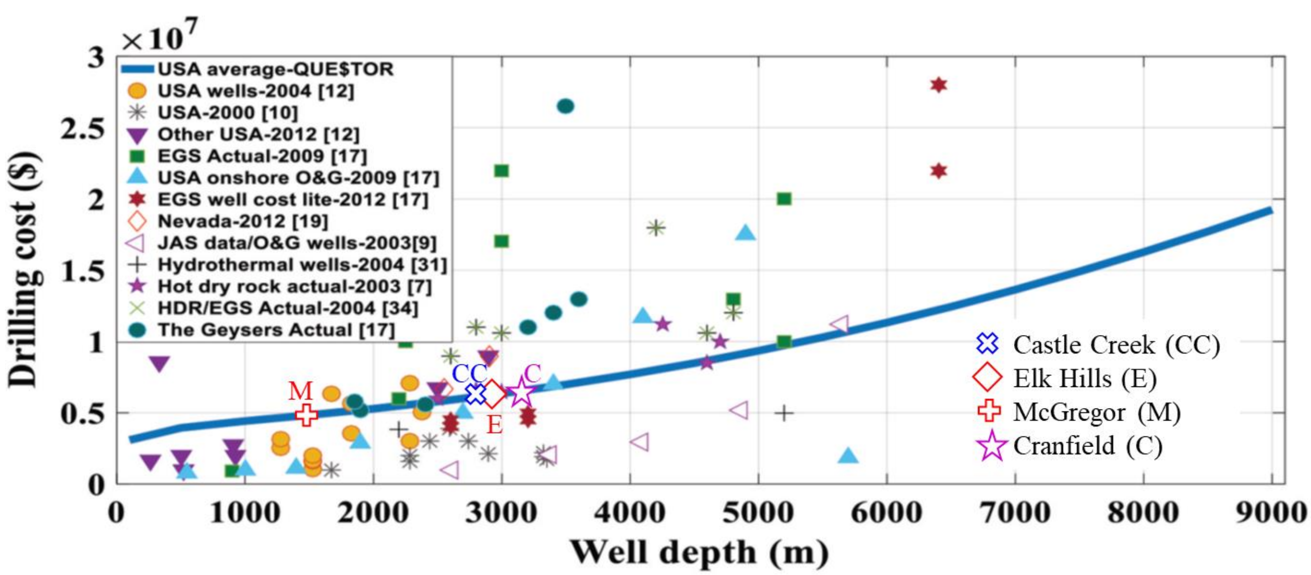

Figure 8. Estimation of drilling cost at four case study sites using a model after Shamoushaki et al. (2021).

4. ESTIMATION OF POWER FOR PRODUCTION AND INJECTION PUMPS

Low and medium temperature geothermal resources require a large flowrate for power generation, that often translates into a large parasitic load for the power plant. Shevenell and McDonald (2014) provide gross and net power generated at the end of 2011 by 21 geothermal power plants in Nevada. Although Shevenell and McDonald (2014) do not specifically mention how the net power was derived, we assumed that the reported generated net power at each site is obtained by subtracting the total parasitic load (e.g., power to run pumps, drive the air-cooled condenser, etc.) from the generated gross power. The analysis of the reported net and gross power of these operational Nevada geothermal power plants yields a total parasitic load in the range of 10-43% of the generated gross power with an average total parasitic load of 26±9%. This calculation shows that the parasitic load can be a significant component of operational cost to geothermal plant operators, and estimation of site-specific parasitic load is important to assess its economic viability.

In this study, we used a method suggested by Banks et el. (2020) to estimate production well pumping power needed to generate 1 MWe at each site. For estimating injection pump power, we used a method based on Adams et al. (2013) and Banks et al. (2020). These estimations assume a non-hybrid (geothermal only) power generation at each of the selected case study sites. Also, the pumping power for production and injection wells discussed here does not include additional parasitic load to operate power plants, cooling fans, moving fluids within the surface infrastructure, etc.

The calculations for both production and injection pump power are presented in Table 4. Different parameters given in Table 4 are successively used to calculate derivative parameters to estimate both production and injection pump power required to generate 1 MWe. In short, the density of water in Table 4 was calculated based on the total dissolved solid content in the brines. The reservoir pressures at the reservoir depth were obtained either from measured data [e.g., from historical well log reports retrieved from California Geologic Energy Management Division (CalGEM) repository (https://filerequest.conservation.ca.gov/wellrecord) for the Elk Hills wells] or using the height of water column from the water table/piezometric surface to the reservoir and back converting them to hydrostatic pressure. Wellhead elevation is the surface elevation (from mean sea level) at the wellhead. Hydraulic head is the water column height from reservoir to the water table/piezometric surface. Injection temperature is the temperature of brine after heat being extracted for generation. The electrical utilization factor (η) at each site was calculated using Equation (1) from Banks et al. (2020). It is noted here that the electrical utilization factor obtained with Equation (1) appears to be higher, almost approaching the Carnot limit. The electrical utilization factor given in Table 4 are significantly higher than the values obtained with endo-reversible approach or with IPSEpro method that we are using for detailed modeling (e.g., Wendt et al., 2023; McTigue et al., 2023; Wendt et al., 2024).

$$\eta = [(0.3083 \times T_r) - 98.794]/100 \qquad (1)$$

where T_r is reservoir temperature in Kelvin.

Table 4. Production and injection pumping power to generate 1 MWe geothermal power at four case study sites.

Site	Well	Depth, m	Water density, kg/m3	Reservoir Pressure, kPa	Wellhead elevation, m	Haudraulic head, m	Reservoir temperature, °C	Injection temperature, °C	Electrical utilization factor (η)	Flow rate for 1 MWe (kg/sec)
Castle Creek	Lawrence D No. 1	2,673	1,102	28,867	836	2,673	108	51	0.19	22
Elk Hills	515-29R	2,818	1,118	23,511	430	2,146	135	52	0.27	11
Fort Bliss	56-5	1,500	1,106	14,654	1,253	1,352	96	51	0.15	35
Cranfield	F2 Well	3,100	1,165	32,000	97	2,803	127	51	0.25	13
Site	Well	Depth to water level (Δh_w), m	Pump power for 1 MWe, Pd (kWe)	Hydraulic head for 5 MPa pressure (m)	Effective hydraulic head for injection (Δh_{wi}), m	Injection wellhead pressure (psi)	Inj pump power for 1 MWe, Id, (kWe)	Total pumping load for 1 MWe (kWe)	Flow per well (gpm)	# of production wells for 10 MWe
Castle Creek	Lawrence D No. 1	0	0	463	463	725	181	181	1000	8
Elk Hills	515-29R	672	125	456	0	0	0	125	1300	4
Fort Bliss	56-5	148	91	461	313	493	193	284	1000	12
Cranfield	F2 Well	297	66	438	141	233	31	98	2000	2

The brine flowrate for the generation of 1 MWe (kg/sec) is obtained by:

$$m = 1000/(\eta \times C_p \times \Delta T) \qquad (2)$$

where C_p is heat capacity of the geothermal brine and assumed to be value of 4.2 kJ/kgK and ΔT is the difference between reservoir temperature and injection brine temperature.

Depth to water level (Δh_w) is the distance from wellhead to the water table/piezometric surface. Since the Castle Creek area is characterized as an artesian system, the depth to water level is assumed to be 0. Finally, the production well pump power (P_d) to generate 1 MWe is obtained by:

$$P_d = -(m \times g \times \Delta h_w)/\xi \qquad (3)$$

where ξ is pump efficiency. In this study we used 0.7 and 0.8 as the mechanical and electrical efficiency for the pump resulting in a net pump efficiency of 0.56.

To estimate the injection pumping power, at least an excess pressure of 5 MPa is assumed to be required to maintain at the reservoir level to facilitate injected brine to flow into the reservoir (Adams et al., 2013). This excess pressure could be generated by mechanical pumps or creating a water column in the wellbore (if the depth to the water table is adequate). For this, we calculated the equivalent water column height (hydraulic head) needed to exert 5 MPa hydrostatic pressure at each site. For the Castle Creek site with an artesian flow, the net excess pressure must be exerted with mechanical pumps. On the other hand, the depth to the water table at the Elk Hills site (672 m) is deeper than the water column (456 m) required to create 5 MPa hydrostatic pressure, the hydraulic head for injection is assumed to be 0. For the McGregor and Cranfield sites, the depths to water table/piezometric surfaces are subtracted to obtain the effective injection hydraulic heads. After the determination of effective injection hydraulic head at each site, Equation 3 is used to calculate injection well pump power (I_d) to inject brine after generation of 1 MWe. The total pumping load for the power plant producing 1 MWe is obtained by summing the power required to produce and inject brines from and to the reservoir. In summary, the pumping load to generate 1 MWe at these sites ranges from 98 kWe to 284 kWe (9.8% to 28.4%). Although Table 4 does not include the parasitic load associated with operation of cooling fans and moving fluid through the plant, the pumping loads at these sites (and total parasitic loads) are likely to appear within the range of parasitic load reported for geothermal power plants in Nevada (Shevenell and McDonald, 2014).

Flow potential per well at different sites in Table 4 are the same values as given in Table 2. The flow rate required for 1 MWe and flow potential per well at each site is upscaled to calculate the number of production wells required to generate 10 MWe at each site. The number of wells required to generate 10 MWe ranged from 2 to 12 wells. It is important to note that the number of wells for power generation given in Table 4 are preliminary, and additional parameters such as productivity of the reservoir need to be evaluated in detail.

5. SUMMARY OF GEO-SOLAR HYBRIDIZATION MODELING RESULTS

The hybrid plant configuration examined in this study uses a steam Rankine topping cycle combined with an organic Rankine cycle (ORC) working fluid-based bottoming cycle. Thermal energy input to the steam cycle is obtained solely from the solar thermal resource. The steam Rankine cycle (SRC) uses a backpressure turbine for power generation. The backpressure turbine exhaust is condensed at a pressure that allows the heat rejected in the steam condensation process to be used for vaporizing the isobutane (iC4) working fluid in the ORC bottoming cycle. While use of the backpressure steam turbine does decrease the power that is generated by the steam Rankine cycle relative to a conventional condensing turbine-based design, the heat rejected from the SRC is transferred to the bottoming ORC to increase the power generation from the ORC. In addition to enabling heat transfer to the bottoming ORC, use of a backpressure steam turbine also decreases the amount of boiler feedwater heating required in the solar-based steam Rankine cycle and allows the hybrid plant to use two thermal energy sources with only a single condenser. The hybrid plant design point performance is maximized for each case study location (each location has a different geothermal resource temperature) by optimizing the ORC turbine inlet pressure. A schematic of the hybrid plant configuration is shown in Figure 9.

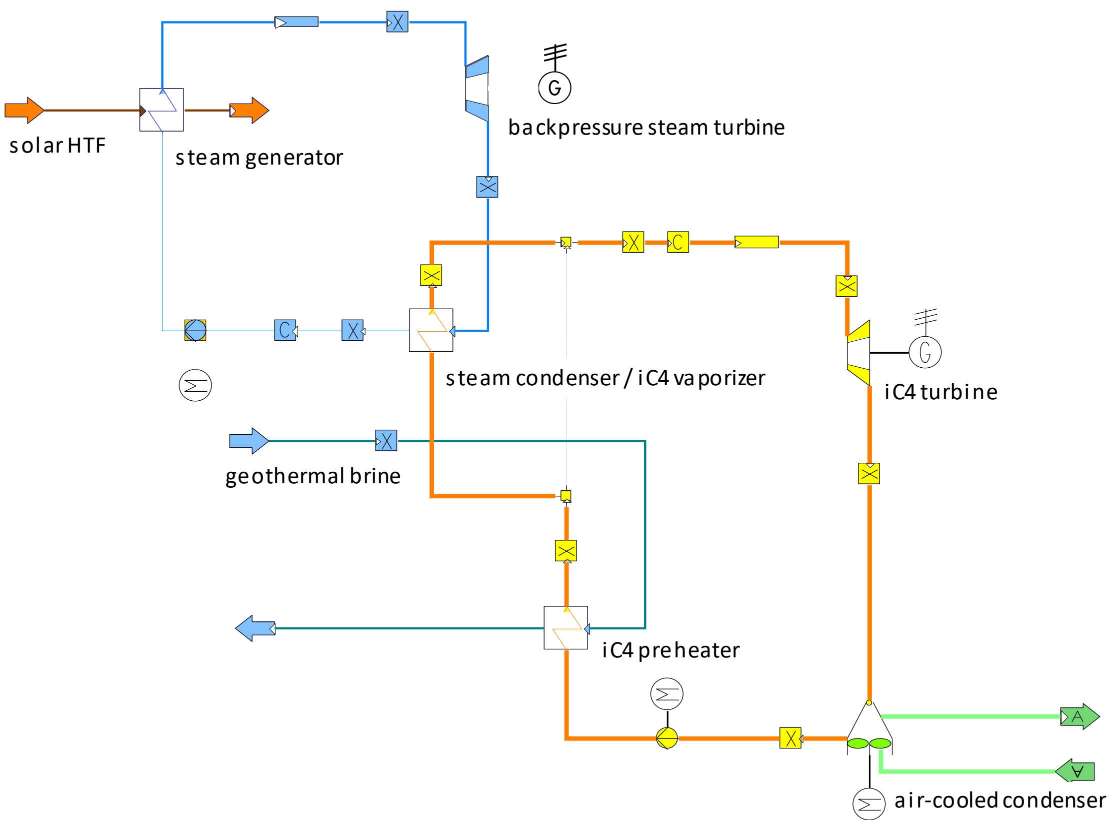

Figure 9. Geo-solar hybrid steam Rankine topping cycle configuration.

Use of the solar heat rejected from the backpressure turbine in the steam Rankine topping cycle to vaporize the ORC bottoming cycle working fluid allows the geothermal heat to be used for preheating the ORC working fluid. This arrangement eliminates the pinch point that is typically encountered when using geothermal brine to vaporize ORC working fluid, which in turn allows maximal heat extraction from the geothermal brine. Since the geothermal resources considered in this analysis are low temperature geothermal resources, it is expected that maximizing the heat extraction from the geothermal brine is a strategy that will allow the most economical use of these resources. Additionally, the use of the geothermal brine to provide the low temperature heat input to the power cycle while using solar heat for the high temperature heat input is a strategy that provides the greatest thermodynamic advantage.

Temperature vs entropy plots for the SRC and ORC are shown in Figure 10. The Figure 10 ORC (right) T-s diagram illustrates that the heat transferred from the geothermal brine is used entirely for sensible heating of the ORC working fluid and does not include a pinch point, and that the heat transferred from the steam cycle turbine exhaust is used entirely for latent heating of the ORC working fluid with a near constant temperature difference between the hot and cold fluid along the length of the heating curve.

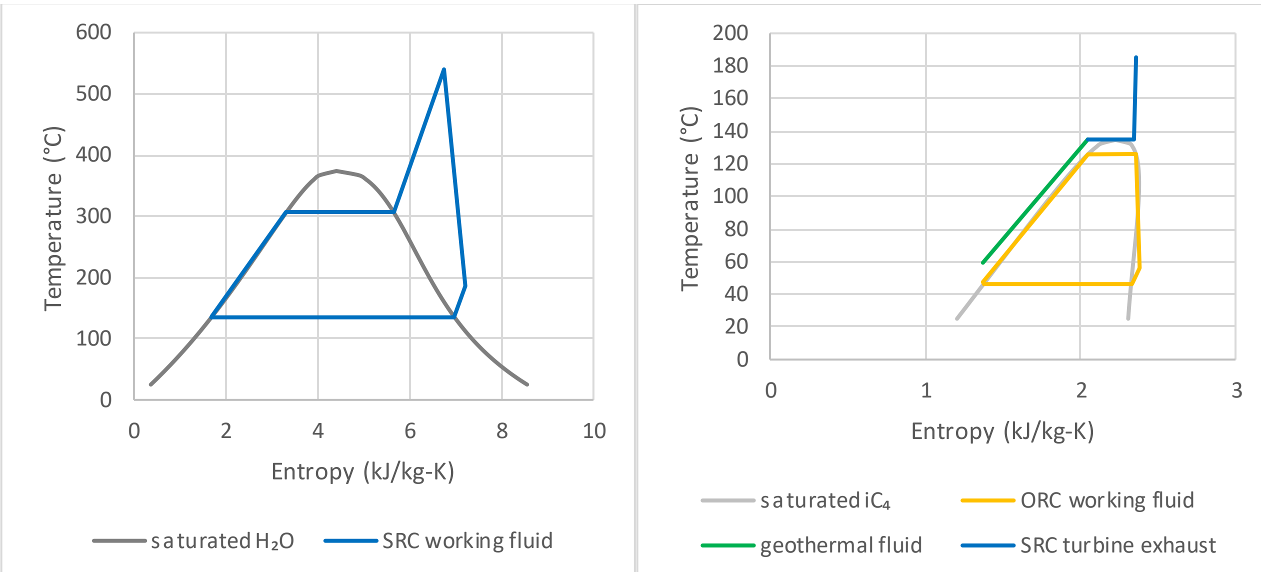

Figure 10. Temperature-entropy diagrams for the hybrid plant steam Rankine cycle (left) and organic Rankine cycle (right)

The hybrid plant design is based on maximal heat input from the solar resource. When the solar resource provides a decreased level of thermal energy, as well as when the ambient temperature deviates from the design condition, the hybrid plant must operate at off-design conditions. The off-design operating strategy includes reducing the ORC turbine inlet pressure to decrease the quantity of solar heat input required to vaporize the iC4 working fluid. When no solar heat is available from the solar collectors or thermal energy storage, the ORC turbine inlet pressure drops to the value that allows all the heat input required to vaporize the iC4 working fluid to be provided by the geothermal brine. The hybrid plant annual power generation was compared against the combined generation from a stand-alone solar thermal plant and stand-alone geothermal plant using the same solar and geothermal resources as the hybrid plant. The stand-alone solar thermal plant configuration used an air-cooled steam Rankine cycle. Several stand-alone geothermal plant configurations were evaluated for each case study location including propane and isobutane working fluid-based single- and dual-pressure level ORCs. Supercritical turbine inlet conditions were specified for case study locations in which the geothermal resource temperature was high enough to enable to support this mode of operation. The isobutane-based dual-pressure ORC provided the greatest stand-alone geothermal plant net power output for each geothermal resource considered and was selected as the baseline geothermal plant against which to compare the hybrid plant performance.

Preliminary power cycle analysis indicates that the annual power generation from the geo-solar hybrid steam Rankine topping cycle exceeds the combined generation from the stand-alone solar thermal and geothermal plants, suggesting that the hybrid plant design may provide the best strategy for utilizing a low-temperature geothermal resource. Future work will include estimation of the hybrid and stand-alone plant capital and operating costs and completion of an economic analysis to determine whether the hybrid plant performance benefits positively impact power generation costs and/or revenues.

6. CONCLUSIONS

Four low to medium temperature geothermal resource locations were selected for evaluation of geo-solar hybrid power plants. The selected locations include Castle Creek, Idaho; Elk Hills, California; McGregor Range, New Mexico; and Cranfield, Mississippi. These locations were selected for their geographic diversity as well as geothermal and solar resource characteristics. These sites provide four unique combinations of high and low solar resources with high (120° C to 150° C) and low (90° C to 120° C) geothermal resources. The Castle Creek location represents low geothermal and low solar resource; the Fort Bliss location represents low geothermal and high solar resource; the Cranfield location represents high geothermal and low solar resource; and finally, the Elk Hills location represents high geothermal and high solar resource.

Geothermal well drilling costs, fluid flow rates, and pumping power requirements were estimated for each of the case study locations. The estimated drilling cost at the Castle Creek, Elk Hills, McGregor, and Cranfield sites are 6.8, 7.0, 4.9, and 7.3 million dollars (2020-dollar value) per well, respectively. The geothermal brine flow rates at the Castle Creek, Elk Hills, McGregor Range, and Cranfield sites are estimated as 1000, 1300, 1000, and 2000 gpm per well with pumping power requirements of 181, 125, 284, and 98 kWe per MWe of stand-alone geothermal plant power generation, respectively.

The steam Rankine topping cycle geo-solar hybrid plant design considered uses solar heat to vaporize the bottoming ORC working fluid so the geothermal heat can be used for preheating the ORC working fluid. This configuration eliminates the pinch point in the geothermal brine to ORC working fluid heat exchanger when operating at the design point to maximize the quantity of heat that is extracted from a low-temperature geothermal resource when compared with a stand-alone geothermal plant. Preliminary power cycle modeling indicates that the geo-solar hybrid plant could provide greater annual power generation than the combined amount from stand-alone plants using equivalent solar and geothermal resources as the hybrid plant. Future work will evaluate the potential for this performance advantage to translate into improved economics when considering the capital and operating costs of the hybrid plant relative to those from the stand-alone plants.

ACKNOWLEDGEMENTS

This work was supported by the United States Department of Energy through Contract No. DEAC07-05ID14517 (INL) and DE-AC36-08GO28308 (NREL). Funding was supplied by the Department of Energy (DOE) Office of Energy Efficiency and Renewable Energy (EERE) Geothermal Technologies Office (GTO).

REFERENCES

Adams, B.M., Kuehn, T.H., Randolph, J.B. and Saar, M.O., 2013. The reduced pumping power requirements from increasing the injection well fluid density. GRC Transactions 37, 667-672.

Adkins, C.B. and Bartolino, J.R., 2012. Historical and Potential Groundwater Drawdown in the Bruneau Area, Owyhee County, Southwestern Idaho. US Department of the Interior, US Geological Survey.

Banks, J., Rabbani, A., Nadkarni, K. and Renaud, E., 2020. Estimating parasitic loads related to brine production from a hot sedimentary aquifer geothermal project: A case study from the Clarke Lake gas field, British Columbia. Renewable Energy, 153, pp.539-552.

Barker, B.J., Nash, G., Moore, J.N. and Bennett, C.N., 2015. Multimodal Geothermal Development in the Tularosa Basin, NM. PROCEEDINGS, Fortieth Workshop on Geothermal Reservoir Engineering, Stanford University, Stanford, California, January 26-28, 2015, SGP-TR-204.

Blackwell, D.D., 1989. Regional implications of heat flow of the Snake River Plain, northwestern United States. Tectonophysics, 164(2-4), pp.323-343.

Brott, C.A., Blackwell, D.D. and Ziagos, J.P., 1981. Thermal and tectonic implications of heat flow in the eastern Snake River Plain, Idaho. Journal of Geophysical Research: Solid Earth, 86(B12), pp.11709-11734.

Doughty, C. and Freifeld, B.M., 2013. Modeling CO_2 injection at Cranfield, Mississippi: Investigation of methane and temperature effects. Greenhouse Gases: Science and Technology, 3(6), 475-490.

Finger, J.T. and Jacobson, R.D., 1997. Fort Bliss exploratory slimholes: Drilling and testing. Report SAND-97-3075, Sandia National Lab. Albuquerque, NM (United States).

Gans, K.D., Metzger, L.F., Gillespie, J.M., and Qi, S.L., 2019. Historical Produced Water Chemistry Data Compiled for the Elk Hills Oilfield, Kern County, California: U.S. Geological Survey data release, https://doi.org/10.5066/P9Z8ZSVS.

Gautier, D.L. and Scheirer, A.H., 2007. Eocene Total Petroleum System—north and east of the Eocene West Side Fold Belt Assessment Unit of the San Joaquin Basin Province, Ch. 19, In: 46 Petroleum Systems and Geologic Assessment of Oil and Gas in the San Joaquin Basin Province, California, USGS Professional paper 1713.

Henry, C.D. and Morton, R.A., 1982. Trans-Boundary Geothermal Resources of Texas and Mexico. Natural Resources Journal, 22, 973-989.

Hosseini, S.A., Lashgari, H., Choi, J.W., Nicot, J.P., Lu, J. and Hovorka, S.D., 2013. Static and dynamic reservoir modeling for geological CO_2 sequestration at Cranfield, Mississippi, USA. International Journal of Greenhouse Gas Control, 18, pp.449-462.

Kharaka, Y.K., Lico, M.S., Law, L.M. and Carothers, W.N., 1981. Geopressured-geothermal resources in California. GRC Transactions, 5, 721-724.

Lear, J., Bennett, C., Lear, D., Jones, P.L., Burdge, M., Barker, B., Segall, M., Moore, J., Nash, G., Jones, C. and Simmons, S., 2016. El Paso County Geothermal Project at Fort Bliss. Final Project Report (No. DE-EE0002827-FINAL). El Paso County, TX (United States).

Lu, J., Kharaka, Y.K., Thordsen, J.J., Horita, J., Karamalidis, A., Griffith, C., Hakala, J.A., Ambats, G., Cole, D.R., Phelps, T.J. and Manning, M.A., 2012. CO2–rock–brine interactions in Lower Tuscaloosa Formation at Cranfield CO2 sequestration site, Mississippi, USA. Chemical Geology, 291, pp.269-277.

Lohse, R.L. and Icerman, L., 1983. Thermal anomaly study for the Otero County area, south central New Mexico. GRC Transaction, 7, 175-180.

Maher, J.C. and Lantz, R.J., 1975. Petroleum geology of Naval Petroleum Reserve No. 1, Elk Hills, Kern County, California. US Geological Survey Professional Paper 912, US Government Printing Office, Washington, p. 118.

Mariner, R.H., Evans, W.C. and Young, H.W., 2006. Comparison of circulation times of thermal waters discharging from the Idaho batholith based on geothermometer temperatures, helium concentrations, and 14C measurements. Geothermics, 35(1), pp.3-25.

McLing, T.L., Dobson, P., Jin, W., Spycher, N., Doughty, C., Neupane, G., Smith, R.W., and Atkinson, T.A., 2022. Dynamic Earth Energy Storage: Terawatt-year, Grid-scale Energy Storage Using Planet Earth as a Thermal Battery (GeoTES): Phase I Project Final Report No. INL/RPT-22-66762. Idaho National Laboratory, Idaho Falls, ID.

McTigue, J.D., Simpson, J.G., Zhu, G., Neupane, G., and Wendt, D., 2023. Design of a geothermal power plant with solar thermal topping cycle. GRC Transactions, 47, p. 12.

Nash, G.D. and Bennett, C.R., 2015. Adaptation of a Petroleum Exploration Tool to Geothermal Exploration: Preliminary Play Fairway Model of Tularosa Basin, New Mexico, and Texas. GRC Transactions, 39, 743-749.

Reid, S.A., 1995. Miocene and Pliocene depositional systems of the southern San Joaquin basin and formation of sandstone reservoirs in the Elk Hills area, California. In Fritsche, A. E., ed., 1995, Cenozoic paleogeography of the western United States—II: Pacific Section, SEPM (Society for Sedimentary Geology), book 75, p. 131-150.

Riestenberg, D. and Gray, K., 2009. Geologic Storage Capacity for CO2 of The Lower Tuscaloosa Group and Woodbine Formations (SECARB Phase III Work Product 1.1 c Final Report) (No. DOE-SSEB-42590-103). Advanced Resources International, Inc, Arlington, VA (United States).

Roy, R., Taylor, B. and Miklas Jr, M.P., 1983. Geothermal exploration in Trans-Pecos, Texas/New Mexico. Final report (No. DOE/ID/12080-T1). Texas Energy and Natural Resources Advisory Council, Austin (USA).

Sanyal, S.K., Robertson-Tait, A., Kraemer, M. and Buening, N., 1993. A survey of potential geopressured resource areas in California (No. SGP-TR-145-3). GeotherEx, Inc., Richmond, CA; California Energy Commission, Sacramento, CA.

Shamoushaki, M., Fiaschi, D., Manfrida, G., Niknam, P.H. and Talluri, L., 2021. Feasibility study and economic analysis of geothermal well drilling. International Journal of Environmental Studies, 78(6), 1022-1036.

Shevenell L. and McDonald B., 2014. Geothermal energy. The Nevada Mineral Industry 2012, Nevada Bureau of Mines and Geology, Special Publication MI-2012, 126-48.

Spycher, N., Doughty, C., Dobson, P., Neupane, G., Smith, R., Jin, W., Atkinson, T. and McLing, T., 2021. Evaluation of mineral scaling during high-temperature thermal energy storage in deep saline aquifers. GRC Transactions, 45, 1201-1215.

Taylor, B., Roy, R.F. and Keller, G.K., 1979. Geothermics in trans-Pecos Texas: Preliminary findings. GRC Transactions, 3, 713-715.

Taylor, B., Roy, R.F. and Hoffer, J.M., 1980. Hueco Tanks: An initial evaluation of a potential geothermal area near El Paso, Texas. GRC Transactions, 4, 253-256.

Wendt, D., Neupane, G., Simpson, J., Zhu, G., and McTigue, J., 2023. Hybrid natural gas geothermal combined cycle power plant analysis. SPE Energy Transition Symposium, SPE-215757, p. 10.

Wendt, D., Neupane, G., Simpson, J., Zhu, G., and McTigue, J., 2024. Techno-Economic Analysis of Solar Topping Cycle Hybrid Geothermal Power Plants for Greenfield Applications. Final Project Report, in preparation. Idaho National Laboratory.

Williams, C.F., Grubb, F.V. and Galanis Jr, S.P., 2004. Geothermal resources of California sedimentary basins. In Geothermal Energy: The Reliable Renewable-Geothermal Resources Council 2004 Annual Meeting. GRC Transactions, 28, 379-383.

Wood, S.H., and Clemens, D.M., 2002. Geologic and tectonic history of the western Snake River Plain, Idaho and Oregon. In Bonnichsen, B., White, C.M, and McCurry, M. (eds.), Tectonic and magmatic evolution of the Snake River Plain volcanic province. Idaho Geological Survey Bulletin 30, 69-103.

Woodring, W.P., Roundy, P.V., and Farnsworth, H.R., 1932. Geology and Oil Resources of the Elk Hills, California: Including Naval Petroleum Reserve No. 1. US Government Printing Office, Washington, p. 102.

Young, H.W. and Lewis, R.E., 1982. Hydrology and geochemistry of thermal ground water in southwestern Idaho and north-central Nevada (No. USGS-PP-1044-J). Geological Survey, Boise, ID (USA).

Young, H.W., and Whitehead, R.L., 1975. Geothermal Investigations in Idaho. Part 2: An evaluation of thermal water in the Bruneau-Grand View area, southwest Idaho. Water Information Bulletin No. 30, Idaho Department of Water Resources, 125 p.